ADVANCED FUNCTIONAL MATERIALS
www.afm-journal.de

Towards van der Waals Epitaxial Growth of GaAs on Si using a Graphene Buffer Layer

Yazeed Alaskar, Shamsul Arafin, Darshana Wickramaratne, Mark A. Zurbuchen, Liang He, Jeff McKay, Qiyin Lin, Mark S. Goorsky, Roger K. Lake, and Kang L. Wang**

Van der Waals growth of GaAs on silicon using a two-dimensional layered material, graphene, as a lattice mismatch/thermal expansion coefficient mismatch relieving buffer layer is presented. Two-dimensional growth of GaAs thin films on graphene is a potential route towards heteroepitaxial integration of GaAs on silicon in the developing field of silicon photonics. Hetero-layered GaAs is deposited by molecular beam epitaxy on graphene/silicon at growth temperatures ranging from 350 °C to 600 °C under a constant arsenic flux. Samples are characterized by plan-view scanning electron microscopy, atomic force microscopy, Raman microscopy, and X-ray diffraction. The low energy of the graphene surface and the GaAs/graphene interface is overcome through an optimized growth technique to obtain an atomically smooth low temperature GaAs nucleation layer. However, the low adsorption and migration energies of gallium and arsenic atoms on graphene result in cluster-growth mode during crystallization of GaAs films at an elevated temperature. In this paper, we present the first example of an ultrasmooth morphology for GaAs films with a strong (111) oriented fiber-texture on graphene/silicon using quasi van der Waals epitaxy, making it a remarkable step towards an eventual demonstration of the epitaxial growth of GaAs by this approach for heterogeneous integration.

1. Introduction

Integration of III-V compound semiconductors on silicon (Si) has been the focus of significant interest over the past 30 years.[1–3] Compared to Si, most IIIV materials have higher carrier mobility, thus making them suitable candidates for high-speed electronic devices. But, due to its cost-effectiveness, chemical stability, and good mechanical strength, Si is still considered the best choice for large-scale integration of microelectronic circuits. III-V materials, however, have direct bandgaps, which is essential for efficient optoelectronic devices, such as light emitting diodes, lasers and photodetectors. Therefore, the integration of III-V materials with Si microelectronics is a burgeoning field with the goal of achieving high speed and efficient optical devices that can be fabricated at a significant performance and cost advantage using standard semiconductor fabrication techniques.

Among several integration methods, direct growth by heteroepitaxy is frequently used to produce the layered structures which in turn are used for device fabrication. Molecular beam epitaxy (MBE) has proven to be a useful tool to grow epifilms with atomically flat surfaces and abrupt interfaces. While nearly perfect homoepitaxial growth was demonstrated by MBE,[4] heteroepitaxial growth is challenged by dissimilar chemical bonding, surface dangling bonds, surface states, and surface symmetry mismatch. In addition, lattice mismatch, polar-on-non-polar epitaxy, and thermal expansion mismatch add complexity to the direct heteroepitaxial growth of GaAs/Si.

Since the first demonstration by Koma on the 2D/2D, for example, selenium/tellurium and $NbSe_2/MoS_2$ material systems in 1984,[5] van der Waals epitaxy (vdWE) has been proven

Y. Alaskar, Dr. S. Arafin, Dr. L. He, Prof. K. L. Wang
Department of Electrical Engineering
University of California at Los Angeles
CA 90095, USA
E-mail: sarafin@ucla.edu; wang@seas.ucla.edu

Y. Alaskar
National Nanotechnology Research Center
King Abdulaziz City for Science and Technology
Riyadh 11442, Saudi Arabia

D. Wickramaratne, Prof. R. K. Lake
Laboratory for Terahertz and Terascale Electronics
University of California at Riverside
CA 92521, USA

Dr. M. A. Zurbuchen, J. McKay,
Prof. M. S. Goorsky, Prof. K. L. Wang
Department of Materials Science and Engineering
University of California at Los Angeles
CA 90095, USA

Dr. M. A. Zurbuchen, Prof. K. L. Wang
California NanoSystems Institute
University of California at Los Angeles
CA 90095, USA

Dr. Q. Lin
Laboratory for Electron and X-ray Instrumentation
University of California at Irvine
CA 92697, USA

DOI: 10.1002/adfm.201400960

 © 2014 WILEY-VCH Verlag GmbH & Co. KGaA, Weinheim

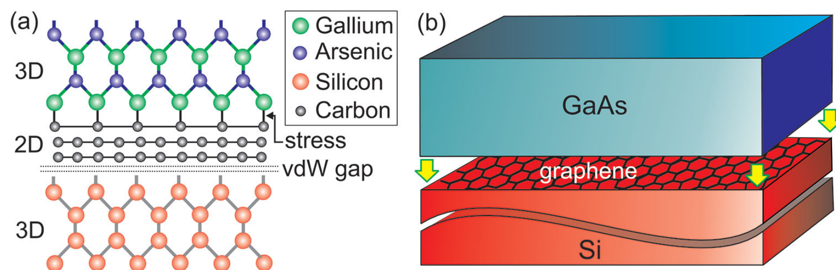

Figure 1. a) Atomic geometry of GaAs/multi-layer graphene/Si interface showing only the top-most graphene layer is strained by heteroepitaxial growth, b) schematic view for a structure with GaAs grown on top of single layer graphene buffer layer/Si substrate.

to be a useful route to heteroepitaxy, alleviating most of the aforementioned constraints. Utilizing such route, depositing a material with three-dimensional (3D) bonding on a two-dimensional (2D) layered van-der-Waals material could be a new and interesting approach of heteroepitaxy. The bonds between the 2D material / upper 3D epilayer in this approach are about two orders of magnitude weaker in comparison to the covalent bonds between the 3D substrate/3D deposited layer. Therefore, the weak bonds between 3D / 2D could accommodate thermal mismatch with different substrate temperatures during the growth. Furthermore, the strain due to the inplane latticemismatch with the epitaxially-grown 3D overlayers is mitigated in quasi-van der Waals Epitaxy (QvdWE)[6] due to low growth-axis bond energies. Considering further, the dislocations at 3D/2D heterointerface are not expected to propagate through the grown material due to such weak interactions. Only the topmost layer of the substrate with 2D nature is expected to undergo a change of its lattice parameters to be isomorphic with the epilayers grown on top due to the van der Waals forces between the layers of the substrate as displayed in **Figure 1**a. Although the stress induced by the interaction between the grown 3D layer and 2D substrate may result in a non-ideal interface, the QvdWE is expected to lead to improved crystalline properties and reduced structural defects such as dangling bonds and dislocations in the grown overlayers.[7]

The QvdW epitaxial growth of GaAs on Si using 2D materials that would act as a buffer layer is proposed in this study. Among other vdW materials, graphene is a thermally-stable material that has a highdecomposition temperature, thus making it an ideal material of choice as a buffer layer. Therefore, an approach using graphene as a buffer layer to facilitate the growth of highquality GaAs/Si films, as illustrated in Figure 1b, shows promise. The atomically flat surface of graphene interacts with the deposited epilayer via van der Waals forces. This reduces the influence of the physical parameters of graphene when forming overlayer nuclei. Given the abundance of high-quality graphene and facile ex-situ transfer to almost any substrate surface, the constraint of twofold epitaxy required for other 2D materials, such as GaSe[8] is circumvented. Furthermore, graphene is a promising substrate for flexible and transparent device applications, due to its excellent optical transparency and electrical conductivity.[9–11] Recently, chemical vapor deposition (CVD) has opened a new path for largescale production of high-quality graphene films.[12] If highquality GaAs films could be grown on Si or any polymeric substrates using graphene buffer layers, this would provide a novel, low-cost, transparent and flexible electrode for a number of potential applications such as solar cells,[13] light emitting diodes,[14] or novel heterostructures.[15]

A number of studies[16,17] have been undertaken to achieve highquality MBE-grown GaAs nanowires (NWs) on a graphene/Si substrate. A mixture of zincblende and wurtzite segments with twins and stacking faults were observed at the bottom of the NWs, whereas the rest of the NW is nearly a defect-free zincblende phase.[16] Additional studies have also demonstrated highdensity, vertical, coaxially heterostructured $InAs/In_xGa_{1-x}As$ NWs, over a wide tunable ternary compositional range, through a seed-free vdWE approach using metal organic chemical vapor deposition (MOCVD) on graphene.[17] Nevertheless, successful operation of NW-based devices is impeded by carrier loss mechanisms, surface-state induced band bending, Fermi level pinning, poor ohmic contacts, and uncontrolled incorporation of n- and p-type dopants. Poor optoelectronic performance due to the aforementioned issues prevents NW-based devices from superseding thin-film based ones.[18] A number of experimental investigations have been reported for the growth of GaAs/Si using layered GaSe.[8,19–21] Unfortunately, significant success has not yet been reported for this approach due to several reasons mentioned in reference.[8]

This paper begins with a discussion on the theoretical calculations associated with the QvdW epitaxial growth of GaAs films on Si using a graphene buffer layer. We then describe the experimental methods and their corresponding results through microstructural characterization of the as-grown GaAs layer. The paper closes with concluding remarks for the GaAs/multilayer graphene/Si system.

2. Theoretical Investigation

2.1. Surface Energy Modification

Ab-initio calculations were conducted to obtain an understanding of the modification of the surface energy of the graphene buffer layer with the inclusion of gallium (Ga) and arsenic (As)prelayer. Detailed descriptions of all ab-initio calculations in this study are included in the Supporting Information. **Figure 2** shows schematic structures with the Ga- (or As) prelayer on graphene used to calculate the surface energy of graphene with the inclusion of a Ga- (or As) prelayer. The surface energy of the substrate σ is defined as

$$\sigma = \frac{[E_{\text{slab}} - \sum N_i \mu_i]}{2A} \quad (1)$$

where E_{slab} is the total energy of the substrate calculated from first principles, μ_i the chemical potential of species i in the slab structure, N_i the number of particles of the i-th element in the slab and A the area of the slab.

© 2014 WILEY-VCH Verlag GmbH & Co. KGaA, Weinheim

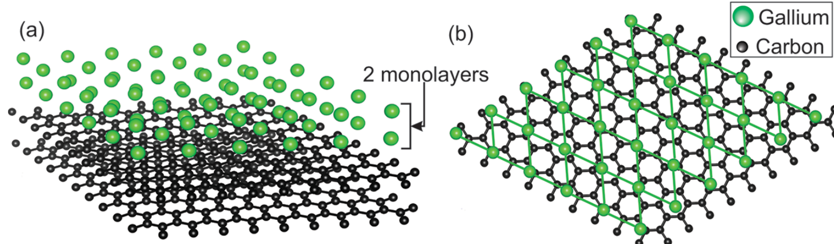

Figure 2. Schematic illustration of optimized supercell with two monolayers of gallium atoms coordinated on bilayer graphene, a) isometric and b) top views of the structure used in our calculation.

The surface energy values calculated for single layer and bilayer pristine graphene along with 3D materials collected from the literature are listed in **Table 1**. The value for the surface energy of graphene is in good agreement with prior experimental reports on the surface energy of graphene.[22,23]

Although graphene atoms have dangling bonds only at the edges and defect sites, ideal graphene is a dangling-bond-free material which results in both the surface energy of graphene and the interface energy between the grown film and the substrate to be negligible. Hence, the growth morphology of the deposited layers can be primarily predicted by the surface energy of only the grown material,[26] that is, GaAs. Therefore, Bauer's surface energy formula for layer-by-layer growth can be simplified as

$$\Delta\gamma \approx \gamma_{\mathrm{GaAs}} \leq 0 \tag{2}$$

where $\Delta\gamma$ is the relative magnitude of the free energy and γ_{GaAs} is the GaAs-vacuum interface energy. 2D materials, such as graphene and Bi_2Se_3, in general, have much lower surface energy compared to 3D materials as can be seen in Table 1. With Ga- and As-prelayer on graphene, the modified σ is calculated to be 0.43 J m^{-2} and 0.57 J m^{-2}, respectively. The predicted order of magnitude increase in the surface energy of the Ga(or As) prelayer/graphene substrate compared to single and bilayer graphene suggests that this increases the wettability of the underlying graphene substrate, thus promoting the likelihood of layer-by-layer epitaxial growth occurring.

2.2. Adsorption and Migration Energy

In addition to the calculations on the modification of the surface energy, we also performed a systematic study of the adsorption and migration energies of Ga, Indium (In), aluminium (Al) and As atoms on graphene in order to have a better understanding of the surface kinetics of these atoms during the growth. VdW interactions were taken into account in our calculations using semi-empirical corrections to the Kohn-Sham energies from DFT. We compared the adsorption energy and bond distance from the nearest carbon atom for the aforementioned elements that are adsorbed on the bridge (B), top (T), and hollow (H) sites (see Figure S1 in Supporting Information) of the bilayer graphene lattice and these results are listed in Table S1. The adsorption energy is calculated using the following expression

$$E_{\mathrm{b}} = E_{\mathrm{supercell}} - E_{\mathrm{atom}} - E_{\mathrm{graphene}} \tag{3}$$

where $E_{\mathrm{supercell}}$ is the total energy per adatom of the 5 × 5 adatom layer on bilayer graphene, E_{atom} is the chemical potential of the adsorbed atom and E_{graphene} is the total energy of the isolated bilayer graphene 5 × 5 supercell. The chemical potential of the adsorbed atoms (Ga, Al, In, As) is calculated with a single atom in a cubic supercell of length 20 Å. Only the Γ point of the Brillouin zone is sampled in this case. The resulting adsorption and migration energies for each of the elements at the most favorable adsorption sites calculated using DFT are summarized in **Table 2**.

The calculation results in Table 2 shows that both Ga and Al have higher adsorption energies compared to As, suggesting to initiate the growth on graphene using either Ga or Al. Despite the higher adsorption energy of Al, its lower migration energy compared to other materials studied could lead to a tendency to form 3D islands, especially at high temperatures. Therefore, among III-As semiconductors, GaAs could be considered the most attractive material in terms of 2D nucleation on graphene. Very recently, the 2D growth of III-nitride on graphene has been demonstrated where nitrogen (N) was used to initiate the

Table 1. Free surface energies of different materials.

Materials	Surface free energy [mJ m^{-2}]
Si (111)	1467[24]
GaAs (111)	1697[24]
Graphene	48
Multi-layer graphene (MLG)	52
Bismuth selenide (Bi_2Se_3)	180[25]

Table 2. Energy and structural properties on the most favorable adsorption sites of Ga, As, In and Al adatoms adsorbed on bilayer graphene. The semi-empirical correction to the vdW forces are applied in conjunction with the LDA functional.

Atom	Favored adsorption site	Adsorption energy E_{b} [eV]	Migration energy E_{m} [eV]
Gallium	H	1.5	0.05
Arsenic	B	1.3	0.21
Indium	H	1.3	0.06
Aluminium	H	1.7	0.03

© 2014 WILEY-VCH Verlag GmbH & Co. KGaA, Weinheim

Table 3. Adsorption energy to bulk cohesive energy ratio of several binary materials, where bulk cohesive energy values are collected from the literature.

Binary materials	Bulk cohesive energy E_c [eV]	Adsorption to bulk cohesive energy ratio $\frac{E_b^{III}+E_b^{V}}{E_c}$
GaAs	6.7[29]	0.4
InAs	6.2[29]	0.42
AlAs	7.7[29]	0.39
GaN	2.2[30]	2.77

growth since nitrogen has both higher adsorption (4.6 eV) and higher migration energy (1 eV) compared to Ga. Nitrogen acts as nucleation sites for the 2D growth of IIInitride films.[27]

A ratio of absorption energy to bulk cohesive energy (E_b/E_c) is another good figure of merit to determine the growth morphology of a compound semiconductor on graphene. Larger ratios will increase the probability of semiconductor adatoms to stick to graphene, and promote the likelihood of 2D growth occuring. Conversely, low ratios will follow a 3D mode since the incident adatoms will tend to stick atop the semiconductor instead of the graphene layer.[28] The bulk cohesive energy (E_c) values of some relevant compound semiconductors collected from the literature are summarized in **Table 3**.

For binary compounds based on the AlGaInAs material system, their E_b/E_c values are very low, hinting that their 2D growth atop graphene is challenging, which agrees well with our experimental results described later. In contrary, a high adsorption to bulk cohesive energy ratio for IIIN materials leads to successful 2D growth on graphene.[31]

3. Experimental Procedure

Multi-layer graphene (MLG) flakes were used as a vdWE buffer layer, and GaAs was deposited on MLG/Si (111) substrates using a Perkin-Elmer 430 MBE system. The MBE system details are provided elsewhere in reference.[32] Material characterization was performed using a fieldemission scanning electron microscope (FESEM, JEOL, JSM-6700F), atomic force microscope (AFM, VEECO Nanoscope IIIa Multimode SPM) in the tapping mode and a double axis X-ray diffractometer (XRD, Bede D1 diffractometer equipped with a Maxflux focusing graded X-ray mirror) with monochromatic CuKα (λ = 1.5405 Å) radiation source. Raman spectra of MLG surfaces and as-grown GaAs films were collected at room temperature (RT) by using a Renishaw Raman microscope with a 532 nm excitation laser.

3.1. Sample Preparation

A 1 cm × 1 cm piece of Si was first rinsed in acetone and isopropanol (IPA) for five minutes. Then, graphene flakes were mechanically exfoliated onto non-HF-treated Si by the well-known scotch-tape technique[33] as shown in **Figure 3**a. Finally

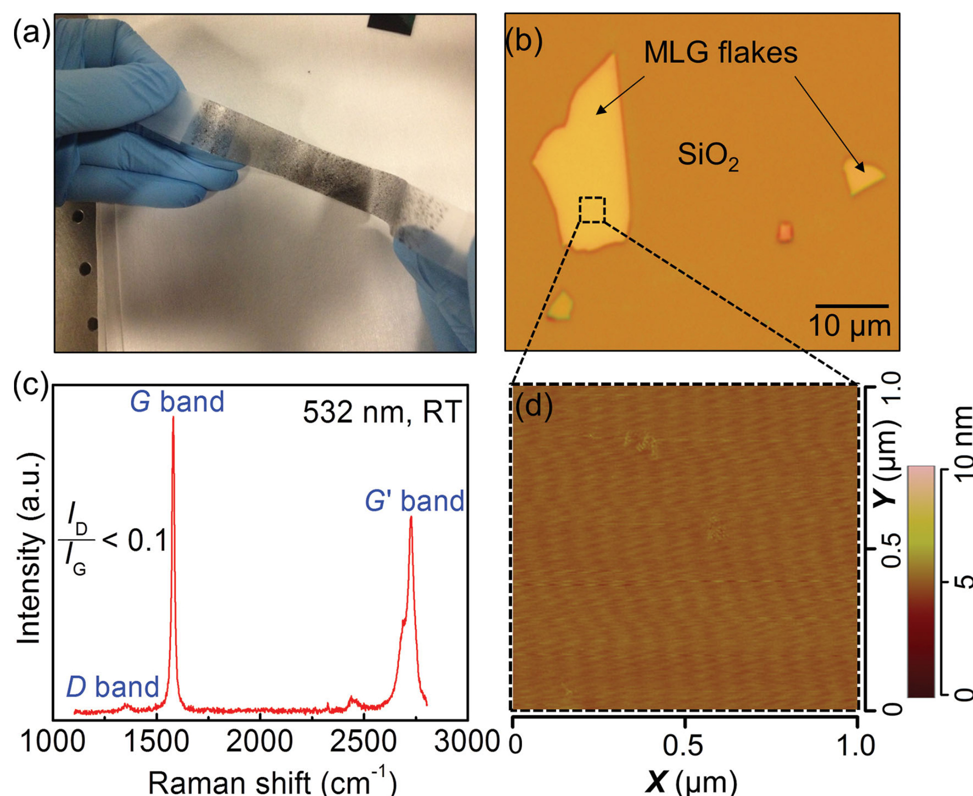

Figure 3. a) Mechanical exfoliation of multi-layer graphene (MLG) flakes using scotch-tape, b) optical microscope image, c) Raman spectrum for the exfoliated MLG, and d) AFM image of the magnified area in b) for the exfoliated MLG on SiO_2/Si showing an ultrasmooth surface morphology.

© 2014 WILEY-VCH Verlag GmbH & Co. KGaA, Weinheim

the Si substrate with MLG was again cleaned using acetone and IPA to remove any residual organics from the exfoliation process. The corresponding microscope image is presented in Figure 3b, showing the MLG flakes onto crystalline Si substrate covered with native SiO_2.

3.2. Graphene Quality

Prior to GaAs growth, it is important to evaluate the quality of the exfoliated MLG layers. This was done by characterizing the crystallinity and surface morphology of MLG flakes using Raman spectroscopy and AFM, respectively. Figure 3c is a Raman spectrum of exfoliated MLG flakes on Si, showing the main features, which are the D, G, and G′ bands. Among these bands, the main peaks are the so-called G and disorder-induced D peaks, which lie at 1580 and 1348 cm^{-1}, respectively. The integrated intensity ratio I_D/I_G for the D band and G band is less than 0.1, indicating high-quality multi-layer graphene.[34] Figure 3d shows the corresponding AFM image for the same MLG flake. The layers exhibit an atomically smooth surface morphology with a peak-to-peak variation of around 0.6 nm and a root-mean-square (RMS) roughness of 0.2 nm.

4. Experimental Results

To achieve high quality epitaxial growth, the nucleation step plays a significant role and influences the film properties, morphology, homogeneity, defect densities, and adhesion. Although the influence of the substrate on nucleation behavior is well understood from convention nucleation theory,[35] there is a limited understanding on the impact of the substrate on the nucleation layer growth in QvdWE. To develop a detailed understanding of the nucleation and growth behavior of GaAs on graphene/Si via QvdWE, GaAs films were grown on MLG using As- or Ga-prelayer, and two-step growth. These grown layers were studied using a combination of SEM, AFM and XRD in order to optimize film quality. Prior to presenting our results, a short description on the preparation for each set of growth conditions will be provided.

4.1. GaAs Growth on As-Terminated MLG Surface

The acetone-IPA-cleaned exfoliated-MLG/Si samples were degassed at 300 °C for 10 min in the buffer tube of our MBE system prior to loading into the growth chamber. The sample was exposed to As flux with a beam-equivalent pressure (BEP) of approximately 1×10^6 Torr. While exposed to the As flux, the substrate temperature was ramped to 400 °C to initiate growth by concurrent introduction of Ga at a nominal growth rate of 0.25 Å/s. After the growth of 25 nm GaAs, the Ga shutter was closed and the substrate was cooled down below 150 °C in the presence of the As flux before unloading.

From a thermodynamic point of view, it is expected that GaAs on MLG/Si system would follow an island mode growth caused mainly by the low surface energy of graphene. From our theoretical investigations described in Section 2, an As-terminated graphene surface will lead to approximately an order-of-magnitude larger surface energy of the graphene surface upon sticking. However, due to their low adsorption energy (i.e., large bond distance) on graphene, As atoms are not found to stick to the graphene surface at high temperatures. Moreover, due to the chemical inertness of the graphene surface, the migration energy of both Ga and As atoms are low at high temperatures. Thus the diffusion length of Ga and As atoms is expected to be very high. Taking this into account, the deposition for the GaAs nucleation layer was performed at temperatures as low as 400 °C to reduce the diffusion length of incident atoms on the graphene. Note that the optimal temperature for GaAs growth is 580–600 °C.[36]

Unfortunately, even this reduced growth temperature fails to prevent the clustering of GaAs into islands atop graphene mainly because of the low migration energy of Ga and As atoms on graphene as mentioned in Section 3. This leads to a poor-quality GaAs film due to island growth in the early stage of nucleation process. **Figure 4**a shows an SEM image of GaAs grown at a V/III ratio of 25 on MLG/Si substrates. According to prior published data,[8] we would still expect that some grains could be epitaxial and their orientations are sensitive to the substrate temperature.

To facilitate the nucleation process or a good anchoring of GaAs atoms on graphene, a second growth was performed with a V/III ratio as low as 10. A lower V/III ratio under otherwise the same growth conditions creates Ga droplets on graphene which act as nucleation sites for the formation of GaAs nanorods (NRs) beside GaAs parasitic crystals, as shown in the SEM image in Figure 4b. These NRs are present in low density on graphene mainly due to the lack of these Ga droplets. Using a Ga-prelayer (i.e. Ga-terminated surface) followed by such a low V/III ratio and a higher growth temperature would increase the number density of these NRs significantly. The length of the NRs is approximately 100 nm, which is much higher than the nominal thickness of the film.

4.2. GaAs Growth on Ga-Terminated MLG Surface

Since Ga has higher adsorption energy on graphene than As,[27] it is expected that the surface diffusion length of Ga and As on graphene will be reduced and the density of nucleation sites for GaAs growth will be increased on the Ga-terminated MLG surface.[37,38] According to our calculations, the surface energy of graphene is increased to 0.43 J m^{-2} from 52 mJ m^{-2} with the introduction of a Ga-prelayer. Thus, we would expect that a further reduction of the growth temperature with Ga- prelayer to increase the wettability of the graphene surface could facilitate the nucleation process.

As part of the optimization of the 2D growth of a GaAs nucleation layer on graphene/Si substrates, a range of Ga-prelayer thicknesses was explored. Approximately two monolayers of gallium atop the graphene surface prior to growth yielded the best results in terms of the surface morphology and material quality, as determined by SEM, AFM and Raman data. In fact, fewer or more than two monolayers of gallium yields a rough GaAs surface (shown in Figure S2 of the Supporting Information) and a low transverse-optic (TO) to longitudinal-optic

© 2014 WILEY-VCH Verlag GmbH & Co. KGaA, Weinheim

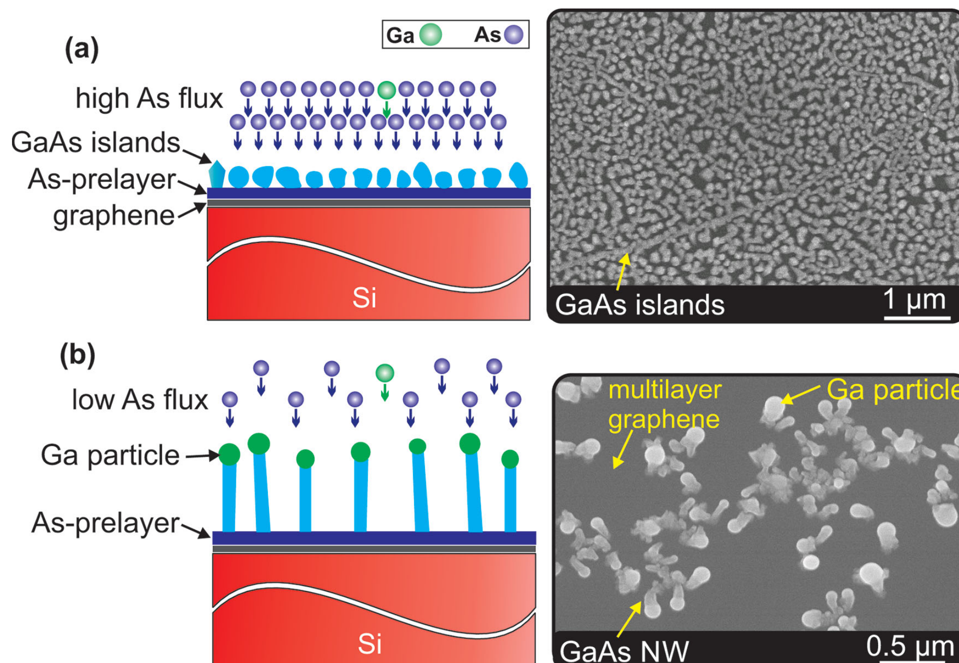

Figure 4. Schematic cross-section views and SEM plan-view images of As-terminated GaAs grown on multilayer graphene/Si with V/III ratios of a) 25 and b) 10 showing island growth and the formation of 1D nanorods, respectively.

(LO) Raman intensity ratio (I_{TO}/I_{LO}).[39,40] It should be noted that such Ga-prelayer deposition was performed at room temperature to achieve a good sticking rate of Ga atoms with graphene, as well as to prevent the Ga clustering observed to occur in higher-temperature depositions. GaAs growth was begun at temperatures as low as 350 °C to avoid islanding and to enhance the nucleation process. This low growth temperature of the nucleation layer was optimized based on the several growth runs. Note that the growth was performed with a V/III ratio of 25, but the growth rate was varied under these conditions.

Figure 5a shows an SEM image of GaAs grown on a Ga-terminated MLG surface at a growth rate 0.25 Å/s. For the first few layers, GaAs forms widely separated islands around nuclei, and then the islands coalesce as the growth proceeds. The extremely thin Ga-prelayer was observed to have a macroscopic effect on the growth of the GaAs nucleation layer. The surface morphology of the structures grown with (Figure 5a) and without (Figure 4a) a Ga-prelayer is noticeably different. This marked difference can be attributed to a difference in the wetting angle between MLG and the upper islands enhancing the 2D nature of growth. Bringans et al. reported that at the initial stage of epitaxy of the GaAs/Si system, a reduction of the wetting angle between the substrate and the overlayer island could be achieved through the use of a Ga-prelayer resulting in a smoother surface morphology.[37] In addition to the effect of Ga-prelayer, the growth rate was also observed to have a significant effect on the surface morphology in 2D growth mode. This is demonstrated in Figure 5b, where a lower growth rate of 0.15 Å/s yielded a smoother GaAs surface. Surface RMS roughnesses as low as 0.6 nm were observed, corresponding to around two monolayers of GaAs, as well as a peak-to-peak height variation of only 3 nm as measured by AFM. This smooth nucleation layer is considered to have an acceptable roughness for subsequent growth of overlayers. To our knowledge, this result is the first illustration of an ultrasmooth morphology for GaAs films on vdW material. This smooth surface could possibly be attributed to a large diffusivity (D) to deposition flux (F) ratio that allows adatoms to reach the surface potential minimum, enhancing a 2D growth of GaAs. In other words, a large value of D/F promotes growth close to an equilibrium condition, allowing the adsorbed species sufficient time to explore the potential energy surface for nucleation so that the system reaches a minimum energy configuration.[41] Hence, the following well-known condition[42] for the step nucleation or layer by layer growth is satisfied by the dimensionless parameter α:

$$\alpha = \frac{Fw^2a^2}{D} < 1 \quad (4)$$

where a is the in-plane lattice constant of graphene and w is the terrace width of exfoliated MLG.

The crystalline quality and the epitaxial orientation of as-grown GaAs films were characterized by Raman spectroscopy and XRD. **Figure 6**a shows the micro-Raman spectrum in which two GaAs Raman signature peaks, corresponding to the TO and LO vibrational bands located at 268 and 292 cm^{-1}, respectively, can be seen. The presence of the forbidden but intense TO-mode in the spectrum is a result of defects in the nucleation layer. The crystallographic quality of this nucleation layer was qualitatively evaluated by I_{TO}/I_{LO} which is observed to be as high as 1.8, indicating incomplete crystallization.

The crystallographic orientation of as-grown GaAs films is mainly defined by the underlying graphene layer, exhibiting triangular lattice symmetry. The silicon substrate will have a negligible influence on the orientation of the grown layer. The

© 2014 WILEY-VCH Verlag GmbH & Co. KGaA, Weinheim

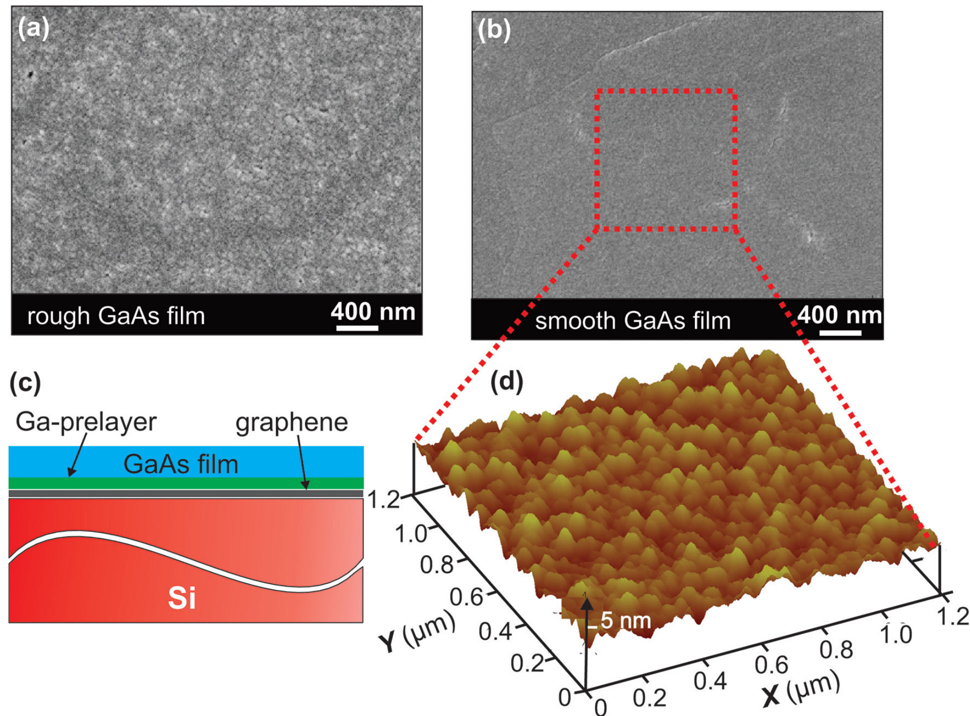

Figure 5. SEM plan-view images of the as-grown structures with a V/III ratio of 25 and at a growth rate of a) 0.25 Å/s, b) 0.15 Å/s, c) schematic cross-sectional view of the GaAs films grown with Ga-prelayer on multilayer graphene/Si, and d) AFM image of the 1.2 μm × 1.2 μm region marked with a red square in (b), showing the surface morphology of the nucleation layer.

crystalline quality for the thin GaAs film on Ga-terminated graphene was characterized by XRD rocking curve scans as shown in Figure 6b. The rocking curve FWHM value for the GaAs(111) plane is 245 arcsec (0.068 deg), indicating that the crystal quality for this orientation requires further improvement. Despite the poor crystal quality, the lowtemperature grown GaAs has a strong (111) oriented fiber-texture. This is clearly an essential step towards demonstration of epitaxy. A clear correlation between the graphene and the fiber texture is confirmed by featureless phi-scan for asymmetric (115) peaks as shown in Figure S3 of the Supporting Information.

Prior reports of the X-ray rocking curves for GaAs on Si[3] show that that a FWHM value of 245 arcsec was attained by employing micron-thick GaAs films. In contrast, our approach achieves the same FWHM with GaAs film thicknesses on the order of 25 nm. The two orders of magnitude improvement in the quality of our GaAs films can be attributed to the graphene buffer layer mitigating lattice and thermal mismatch between GaAs and the underlying substrate.

4.3. GaAs Growth on MLG via Two-Step Growth

Two-step growth processes have already been proven to be a successful approach to deposit GaAs on Si.[43,44] This concept could also be applied in our QvdWE where a good-quality

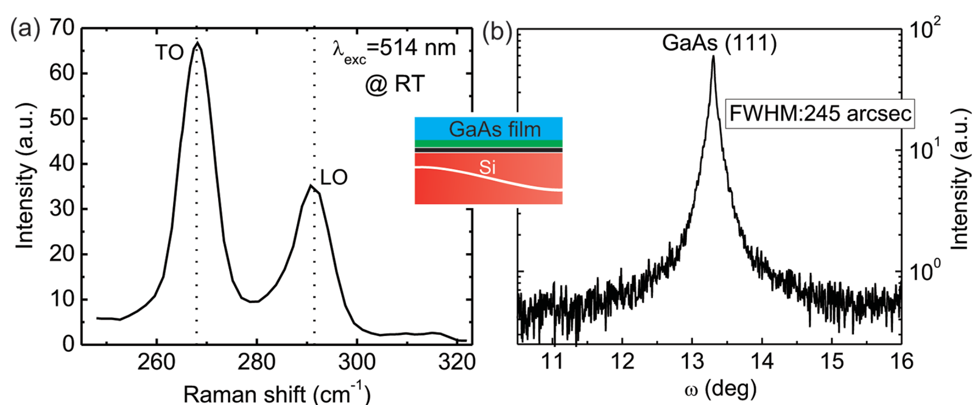

Figure 6. a) The room-temperature micro-Raman spectrum for the low-temperature-grown GaAs nucleation layer, and b) the XRD rocking-curve scan of GaAs(111) peak for such nucleation layer.

© 2014 WILEY-VCH Verlag GmbH & Co. KGaA, Weinheim

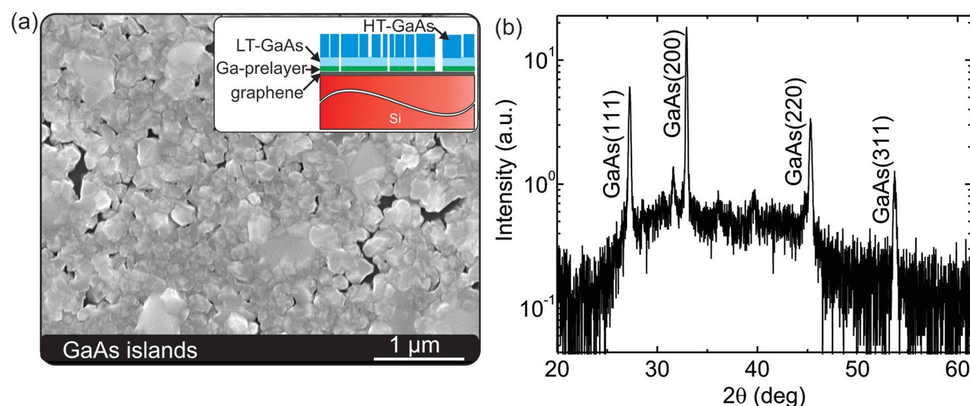

Figure 7. SEM plan-view image of a) 200 nm high-temperature grown GaAs on top of a 25nmthick nucleation layer, with Ga-prelayer showing a 3D cluster growth which could be caused by the elevated temperature during the second step growth and b) XRD $\omega/2\theta$ scan for GaAs grown by the two-step growth scheme, showing polycrystallinity with the presence of GaAs (111), (200), (220), and (311).

nucleation layer is formed at low temperature before high-temperature deposition of crystalline films. Achieving single crystalline GaAs on top of a graphene layer using a one-step growth process is challenging due to difficulties in obtaining a high-quality nucleation layer at a higher temperature. Such challenges stem primarily from a reduced adsorption and migration energy of incident atoms as well as the weak vdW forces that govern the interaction between graphene and GaAs at high temperatures.

After achieving a smooth nucleation layer of GaAs on MLG/Si (see Figure 5b), the substrate temperature was raised to 600 °C, the growth temperature of crystalline GaAs, for a second step growth at the top of the nucleation layer. The second step growth was performed at 1 Å/s and V/III ratio of 100, resulting in a film of 200 nm thick. **Figure 7**a shows the SEM image of the GaAs after the two-step growth. We note that the clearly faceted morphology of the GaAs grains of the film indicate its untextured, polycrystalline nature which is confirmed by the multiple diffraction peaks from (111), (200), (220), and (311) crystal planes in XRD $\omega/2\theta$ scan as shown in Figure 7b. The rough surface morphology of the GaAs after the second step growth also indicates that the underlying nucleation layer is insufficiently stable at the second-stage temperature. To confirm this finding, a nucleation layer was characterized by SEM after raising its temperature to 600 °C without further growth, as displayed in Figure S4 of the Supporting Information.

In order to avoid island growth during the temperature ramp-up in the two-step process, a growth was performed with a low-temperature nucleation layer as thick as 100 nm. Even this failed to prevent island formation. This suggests the GaAs/graphene interface is not stable at high temperatures. Such islanding of GaAs at high temperatures could be mainly caused by the low migration energy of Ga and As atoms on graphene that continues to decrease with increasing temperature. This results in the adatom diffusion at low temperatures or even near room temperature. The low adsorption energy of Ga and As atoms on graphene also indicates a physical adsorption-like bonding, that is, weak interaction between graphene and the adatoms. Moreover, the weakening of the physical vdW bonding with increasing temperature could also be a possible mechanism of island formation. High growth temperatures are required to crystallize GaAs and for the defects and dislocations to migrate in order to obtain high quality GaAs. Unfortunately, in GaAs/graphene, the weak vdW forces that bond GaAs to graphene can be broken at high temperatures. A carefully optimized two-step growth process is essential to form a high-quality nucleation layer at low temperatures followed by a temperature ramp-up that crystallizes the grown GaAs film.

5. Growth Model

Our model of the growth process of GaAs on MLG/Si is shown schematically in **Figure 8**. After the mechanical exfoliation of MLG layer on to the silicon substrate, the QvdWE process begins either with a Ga- or As- prelayer. With a Ga-prelayer, Ga atoms impinge on the room temperature MLG/Si surface to reduce the hopping rate of Ga atoms and to facilitate Ga atoms sticking on the graphene uniformly (Figure 8(ii)-A). With an As-prelayer, the MLG layer is terminated with As atoms at 400 °C. Although the Ga-terminated graphene has a lower surface energy, it is preferred over the As terminated graphene surface (Figure 8(ii)-B). This is because the As atoms do not adhere sufficiently to the graphene surface due to its lower adsorption energy compared to Ga, resulting in an island growth mode when both Ga and As are introduced for GaAs deposition at 400 °C (Figure 8(iii)-B). On the other hand, the growth temperature of 350 °C determined as the optimum for the approach with the Ga-prelayer facilitates GaAs nucleation on an otherwise inert graphene surface where the diffusion length of adatoms is high. When Ga and As atoms are introduced at 350 °C, they both nucleate around Ga sites to form islands. As the growth proceeds, the islands coalesce and eventually form a smooth film (Figure 8(iii)-A). This film adheres to the graphene via vdW forces. For the small flakes characterized in our study, the strain at the interface is believed not to propagate from the interface which limits the lattice mismatch and thermal expansion mismatch at the interface. Raising the temperature of this film to 600 °C causes GaAs to recrystallize into islands by breaking the weak vdW forces between graphene and GaAs (Figure 8(iv)).

© 2014 WILEY-VCH Verlag GmbH & Co. KGaA, Weinheim

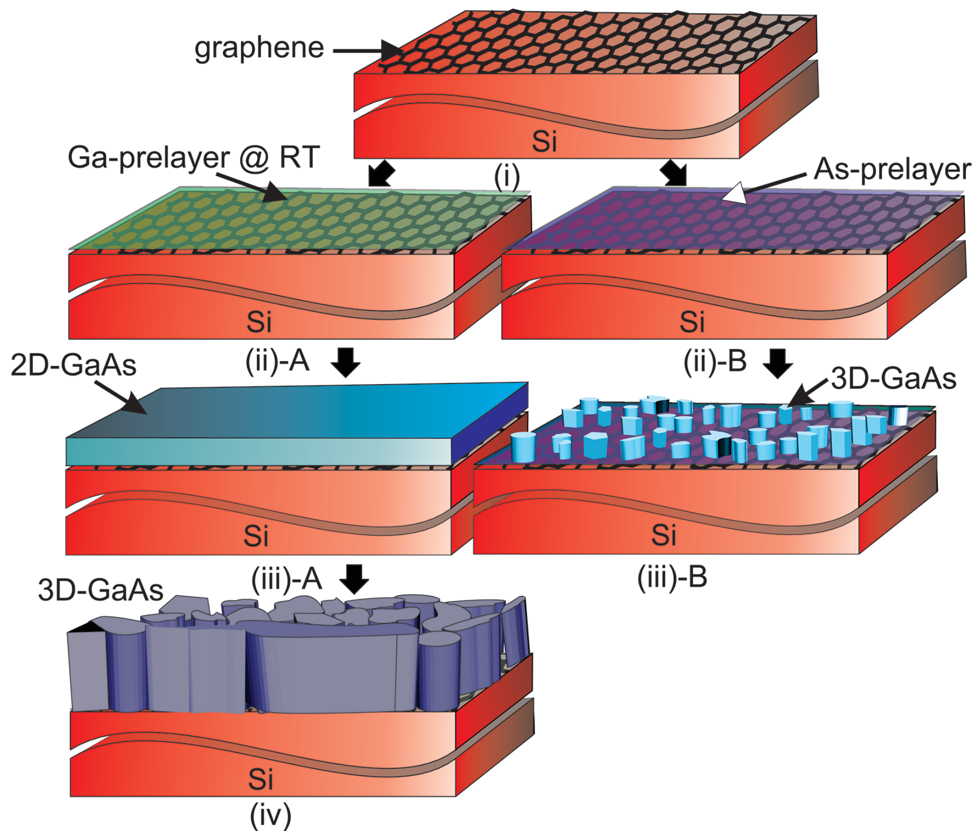

Figure 8. Schematic illustrations of the growth of GaAs on Si via QvdWE at different stages, i) mechanical exfoliation of multi-layer graphene on Si substrate, ii) growth initialization by covering the MLG surface either with Ga- orAs-prelayer, iii) deposition of GaAs nucleation layer, and iv) deposition of GaAs at 600 °C exhibiting a rough surface morphology with 3D islands.

6. Discussion

For the technologically important GaAs/Si heteroepitaxial system, a novel growth concept, QvdWE using graphene as a thermal/lattice mismatch buffer layer has been proposed. This growth mechanism differs from conventional MBE heteroepitaxy due to the use of a 2D buffer material in between the substrate and the overlayers. Such buffers have strong bonding within a layer but weak bonding between vdW layers. We have shown how a smooth 2D GaAs thin film can be formed on the MLG/Si system via QvdWE. Upon thermal annealing to 600 °C and during the deposition of high-temperature GaAs, the growth proceeds by the island growth mode. Although this QvdWE using 2D buffer layers has opened a new window for potentially heteroepitaxial GaAs/Si, some major challenges remain.

i) Surface energy: Due to low surface energy, 2D materials exhibit a high surface tension, so deposited GaAs films will tend not to wet the buffer surface, resulting in island growth, which is empirically associated with high defect densities.

ii) Low adsorption and migration energy: As shown in Table 2, Al, Ga, In, As atoms for the AlGaInAs material system exhibit very low adsorption and migration energies on graphene and thus makes it difficult for GaAs to be stable atop a graphene surface. Thus the 2D growth of IIIAs materials on graphene remains an open challenge.

This study is a first step in the direction of achieving of high-quality single crystal GaAs that takes the advantage of vdW epitaxy using graphene. The results obtained from this study can be used to optimize epitaxial thin film growth of other IIIV semiconductors, for example, InP, GaSb on Si using graphene buffer layers. Further optimization of the growth parameters, such as the right prelayer material on graphene or the use of other candidate van-der-Waal materials are possible ways to integrate single-crystal 2D GaAs on Si. Future efforts will focus on using a low-temperature or a modified deposition technique that would eliminate the occurrence of 3D island growth at high growth temperatures.

Supporting Information

Supporting Information is available from the Wiley Online Library or from the author.

Acknowledgements

Y.A. and S.A. contributed equally to this work. This work is financially supported by the King Abdulaziz City for Science and Technology (KACST), Saudi Arabia under contract number # 20092383 and Center of Excellence for Green Nanotechnology (CEGN). This work also uses the Extreme Science and Engineering Discovery Environment (XSEDE),

© 2014 WILEY-VCH Verlag GmbH & Co. KGaA, Weinheim

FULL PAPER

which is supported by National Science Foundation grant number OCI-1053575. D.W. and R.K.L acknowledge the support from FAME, one of six centers of STARnet, a semiconductor Research Corporation Program sponsored by MARCO and DARPA.

Received: March 25, 2014
Revised: May 11, 2014
Published online: August 26, 2014

[1] W. I. Wang, *Appl. Phys. Lett.* **1984**, *44*, 1149.
[2] M. Yamaguchia, *J. Mater. Res.* **1991**, *6*, 376.
[3] Y. B. Bolkhovityanov, O. P. Pchelyakov, *Open Nanosci. J.* **2009**, *3*, 20.
[4] M. Naganuma, K. Takahashi, *Phys. Stat. Sol.* **1975**, *31*, 187.
[5] A. Koma, K. Sunouchi, T. Miyajima, *Microelectron. Eng.* **1984**, *2*, 129.
[6] Growth of 3D materials on 2D substrates.
[7] W. Wang, K. K. Leung, W. K. Fong, S. F. Wang, Y. Y. Hui, S. P. Lau, Z. Chen, L. J. Shi, C. B. Cao, C. Surya, *J. Appl. Phys.* **2012**, *111*, 093520.
[8] J. E. Palmer, T. Saitoh, T. Yodo, M. Tamura, *J. Appl. Phys.* **1993**, *74*, 7211.
[9] K. S. Novoselov, Z. Jiang, Y. Zhang, S. V. Morozov, H. L. Stormer, U. Zeitler, J. C. Maan, G. S. Boebinger, P. Kim, A. K. Geim, *Science* **2007**, *315*, 1379.
[10] R. H. Kim, M. H. Bae, D. G. Kim, H. Cheng, B. H. Kim, D. H. Kim, M. Li, J. Wu, F. Du, H. S. Kim, S. Kim, D. Estrada, S. W. Hong, Y. Huang, E. Pop, J. A. Rogers, *Nano Lett.* **2011**, *11*, 3881.
[11] C. H. Lee, Y. J. Kim, Y. J. Hong, S. R. Jeon, S. Bae, B. H. Hong, G. C. Yi, *Adv. Mater.* **2011**, *23*, 4614.
[12] S. Bae, H. Kim, Y. Lee, X. Xu, J.-S. Park, Y. Zheng, J. Balakrishnan, T. Lei, H. R. Kim, Y. I. Song, Y.-J. Kim, K. S. Kim, B. Özyilmaz, J.-H. Ahn, B. H. Hong, S. Iijima, *Nat. Nanotechnol.* **2010**, *5*, 574.
[13] M. D. Kelzenberg, S. W. Boettcher, J. A. Petykiewicz, D. B. Turner-Evans, M. C. Putnam, E. L. Warren, J. M. Spurgeon, R. M. Briggs, N. S. Lewis, H. A. Atwater, *Nat. Mater.* **2010**, *9*, 239.
[14] K. Chung, C. H. Lee, G. C. Yi, *Science* **2010**, *330*, 655.
[15] G.-H. Lee, Y.-J. Yu, X. Cui, N. Petrone, C.-H. Lee, M. S. Choi, D.-Y. Lee, C. Lee, W. J. Yoo, K. Watanabe, T. Taniguchi, C. Nuckolls, P. Kim, J. Hone, *ACS Nano* **2013**, *7*, 7931.
[16] A. M. Munshi, D. L. Dheeraj, V. T. Fauske, D. C. Kim, A. T. van Helvoort, B. O. Fimland, H. Weman, *Nano Lett.* **2012**, *12*, 4570.
[17] P. K. Mohseni, A. Behnam, J. D. Wood, C. D. English, J. W. Lyding, E. Pop, X. Li, *Nano Lett.* **2013**, *13*, 1153.
[18] S. Arafin, X. Liu, Z. Mi, *J. Nanophoton.* **2013**, *7*, 074599.
[19] J. E. Palmer, T. Saitoh, T. Yodo, M. Tamura, *Jpn. J. Appl. Phys.* **1993**, *32*, 1126.
[20] J. E. Palmer, T. Saitoh, T. Yodo, M. Tamura, *Mat. Res. Soc. Symp. Proc.* **1994**, *326*, 33.
[21] J. E. Palmer, T. Saitoh, T. Yodo, M. Tamura, *J. Cryst. Growth* **1995**, *150*, 685.
[22] S. Wang, Y. Zhang, N. Abidi, L. Cabrales, *Langmuir* **2009**, *25*, 11078.
[23] Y. J. Shin, Y. Wang, H. Huang, G. Kalon, A. T. Wee, Z. Shen, C. S. Bhatia, H. Yang, *Langmuir* **2010**, *26*, 3798.
[24] A. Zdyb, J. M. Olchoik, M. Mucha, *Mater Science-Poland* **2006**, *24*, 1109.
[25] X. He, W. Zhou, Z. Y. Wang, Y. N. Zhang, J. Shi, R. Q. Wu, J. A. Yarmoff, *Phys. Rev. Lett.* **2013**, *110*, 156101.
[26] W. Jaegermann, A. Klein, C. Pettenkofer, in *Electron Spectroscopies Applied to Low-Dimensional Materials*, Vol. 24 (Eds: H. P. Hughes, H. I. Starnberg), Springer, Netherlands **2002**, Ch. 7.
[27] K. Nakada, A. Ishii, in *Graphene Simulation*, (Ed: J. R. Gong), InTech, Rijeka, Croatia **2011**, Ch. 1.
[28] X. Liu, C.-Z. Wang, M. Hupalo, H.-Q. Lin, K.-M. Ho, M. Tringides, *Crystals* **2013**, *3*, 79.
[29] A. Aresti, L. Garbato, A. Rucci, *J. Phys. Chem. Solids* **1984**, *45*, 361.
[30] H. Morko, in *Handbook of Nitride Semiconductors and Devices*, Vol. 1, Wiley-VCH Verlag GmbH & Co. KGaA, Weinheim, Germany **2008**.
[31] P. Gupta, A. A. Rahman, N. Hatui, M. R. Gokhale, M. M. Deshmukh, A. Bhattacharya, *J. Cryst. Growth* **2013**, *372*, 105.
[32] G. Huang, F. Xiu, B. F. Alsubaie, L. He, X. Kou, X. Yu, K. L. Wang, M. S. BenSaleh, A. A. Alatawi, presented at *Conf. Proc. IEEE SIECPC'11*, Riyadh, Saudi Arabia **2011**.
[33] A. K. Geim, *Science* **2009**, *324*, 1530.
[34] A. C. Ferrari, *Solid State Commun.* **2007**, *143*, 47.
[35] B. Lewis, J. C. Anderson, *Nucleation and Growth of Thin Films*, Academic Press, New York, NY, USA **1978**.
[36] S. C. Lee, L. R. Dawson, S. R. J. Brueck, A. Stintz, *J. Appl. Phys.* **2004**, *96*, 4856.
[37] R. D. Bringans, M. A. Olmstead, F. A. Ponce, D. K. Biegelsen, B. S. Krusor, R. D. Yingling, *J. Appl. Phys.* **1988**, *64*, 3472.
[38] R. D. Bringans, M. A. Olmstead, R. I. G. Uhrberg, R. Z. Bachrach, *Appl. Phys. Lett.* **1987**, *51*, 523.
[39] R. J. Matyi, W. M. Duncan, H. Shichijo, H. L. Tsai, *Appl. Phys. Lett.* **1988**, *53*, 2611.
[40] S. W. da Silva, D. I. Lubyshev, P. Basmaji, Yu. A. Pusep, P. S. Pizani, J. C. Galzerani, R. S. Katiyar, G. Morell, *J. Appl. Phys.* **1997**, *82*, 6247.
[41] J. V. Barth, G. Costantini, K. Kern, *Nature* **2005**, *437*, 671.
[42] A. K. Myers-Beaghton, D. D. Vvedensky, *Phys. Rev. B* **1990**, *42*, 5544.
[43] M. Akiyama, Y. Kawarada, T. Ueda, S. Nishi, K. Kaminishi, *J. Cryst. Growth* **1986**, *77*, 490.
[44] C. W. Hsu, Y. F. Chen, Y. K. Su, *Nanotechnology* **2012**, *23*, 495306.

© 2014 WILEY-VCH Verlag GmbH & Co. KGaA, Weinheim